frontiers | Frontiers in Environmental Science

TYPE Original Research
PUBLISHED 08 May 2025
DOI 10.3389/fenvs.2025.1591564



OPEN ACCESS

EDITED BY
Qi Liao,
Central South University, China

REVIEWED BY
Shan Zhong,
Jiangsu University, China
Dr V. N. Meena Devi,
Noorul Islam University, India

*CORRESPONDENCE
Youbin Si,
youbinsi@ahau.edu.cn

RECEIVED 11 March 2025
ACCEPTED 25 April 2025
PUBLISHED 08 May 2025

CITATION
Chen Q, Min Q, Wu H, Zhang L and Si Y (2025) Biomineralization of $Cd^{2+}$ and $Pb^{2+}$ by sulfate-reducing bacteria *Desulfovibrio desulfuricans* and *Desulfobulbus propionicus*. *Front. Environ. Sci.* 13:1591564. doi: 10.3389/fenvs.2025.1591564



# Biomineralization of $Cd^{2+}$ and $Pb^{2+}$ by sulfate-reducing bacteria *Desulfovibrio desulfuricans* and *Desulfobulbus propionicus*

Qianyanyu Chen, Qi Min, Hui Wu, Li Zhang and Youbin Si*

Anhui Province Key Laboratory of Farmland Ecological Conservation and Pollution Prevention, College of Resources and Environment, Anhui Agricultural University, Hefei, China

Sulfate reducing bacteria (SRB) is considered to be the most promising alternative biological treatment for immobilization of heavy metals due to its high efficiency and low cost. However, the mechanism underlying the biomineralization process has remained unclear. In this study, the kinetics and effects of Cd2+ and Pb2+ mineralization by sulfate-reducing bacteria Desulfovibrio desulfuricans and Desulfobulbus propionicus were investigated based on the microbial treatment technology, and the scanning electron microscope and energy dispersive spectroscopy (SEM-EDS), transmission electron microscope (TEM), X-ray diffractometer (XRD), Raman spectra and X-ray photoelectron spectroscopy (XPS), were used to reveal the mechanism of SRB treatment. The results showed that D. propionicus had a more efficient heavy metal mineralization rate than the D. desulfuricans, up to 98.97% and 75.62% at initial Cd2+ concentrations of 30 and 60 mg/L particularly. respectively. Both D. desulfuricans and D. propionicus had achieved 80% immobilization efficiency of Pb2+ with an initial Pb2+ concentration less than 50 mg/L. D. desulfuricans and D. propionicus facilitate the precipitation of Cd2+ and Pb2+ in the solution primarily as CdS, while Pb were mineralized and removed through phosphate and oxide precipitates of Pb and PbS via their metabolic activities involving sulfate conversion. This research suggested that mineralization of heavy metals mediated by microbial sulfate reduction should have prospects for broad application in bioremediation of mine drainage.

KEYWORDS

**Desulfovibrio desulfuricans, Desulfobulbus propionicus, microbial sulfate reduction, $Cd^{2+}$, $Pb^{2+}$, biomineralization**

## 1 Introduction

With industrial modernization, large volumes of wastewater containing heavy metals and sulfate are released into the natural environment, resulting in serious pollution (Alam et al., 2024; Rehman et al., 2025b). High concentrations of heavy metals in the vicinity of mines are harmful to groundwater, which hinders the development of agriculture and creates quantitative and qualitative problems in grain production(Ahluwalia and Goyal, 2007; Gramp et al., 2010; Xu H. et al., 2021). Among heavy metal contaminants, cadmium, lead and arsenic are the most prevalent (Zheng et al., 2024a). When heavy metals reach human tissues through various absorption pathways, such as direct ingestion, skin contact or absorption through food chain, they will have serious impacts on human health(Southam and Saunders, 2005; Thatoi et al., 2014).

Currently, various treatment technologies such as chemical precipitation, coagulation/flocculation, ion exchange, adsorption, membrane filtration, or electrocoagulation, etc., have been developed for the remediation of heavy metal pollution in environment (Liao et al., 2024; Zheng et al., 2024b; Rehman et al., 2025a). Despite the progress achieved by these conventional methods, they have notable drawbacks, such as high operational costs and the potential generation of secondary pollutants, which may exacerbate environmental harm (Hu et al., 2024). In contrast, the microbial remediation of heavy metals is widely utilized by scientists due to its high cost-effectiveness, environmental friendliness, and simplicity of operation. Microorganisms have the capability to alter the form of heavy metals present in the environment by influencing their chemical or physical properties (Liao et al., 2024). In particular, the sustainable bioremediation technology based on sulfate-reducing bacteria (SRB) is considered to be one of the best treatment schemes to alleviate environmental pollution caused by heavy metals. SRB can reduce sulfate, sulfite, thiosulfate and other sulfur oxides and elemental sulfur to hydrogen sulfide. It can not only adapt to various extreme environments, but also play an important role in the geochemical sulfur cycle (Liu et al., 2013; Le Pape et al., 2017).

At present, there are some reports on the use of sulfate-reducing bacteria for removing heavy metals from wastewater (Wang et al., 2014; Siswoyo et al., 2019). However, there are many confounding factors that need to be considered, which add difficulties for the remediation of heavy metal mine drainage by sulfate reducing bacteria. The environmental conditions, including pH, temperature, and heavy metal toxicity, significantly influence the activity of sulfate-reducing bacteria (SRB) and their efficiency in metal fixation (Liao et al., 2024). The optimal pH for SRB growth typically ranges between 5 and 9, with peak activity observed at 6.5–7.1, as extreme pH levels disrupt metabolic functions—lower pH (<5) leads to protonation of active sites, competition between $H^+$ and metal cations for binding sites, and increased solubility of toxic $Cd^{2+}$, while higher pH (>9) inhibits growth and sulfate reduction (Hu et al., 2024). Additionally, temperature plays a critical role, as SRB thrive at 28°C–32°C; low temperatures reduce membrane fluidity, protein stability, and substrate affinity, whereas high temperatures increase membrane permeability and risk cell lysis, despite enhancing biochemical reaction rate (Diao et al., 2023; Liao et al., 2024). Heavy metals, such as Cu and Zn, further inhibit SRB by disrupting enzyme function through binding to thiol groups or displacing cofactors, leading to growth suppression, metabolic slowdown, delayed sulfide production, and microbial decay. The presence of multiple heavy metals can exacerbate toxicity due to synergistic effects, though competing inorganic cations may mitigate some metal toxicity by occupying anionic cell surface sites(Zhang et al., 2022). Collectively, these factors underscore the need for optimized environmental conditions to maximize SRB-mediated metal immobilization. Currently, the accepted traditional techniques for remediation of heavy metal mine drainage are often too expensive for practical application, and often fail to restore their physical and chemical properties (Lee and Hur, 2016; Picard et al., 2018).Therefore, microbial mineralization, as a cost-effective and eco-friendly technology, is currently the most suitable method to deal with heavy metal pollution (Roychoudhury et al., 2003; Meulepas et al., 2009; Somenahally et al., 2011).

The basic principle of microbial sulfate reduction mediated heavy metal mineralization is that sulfate-reducing bacteria use sulfate as electron acceptor and organic matter as carbon source and electron donor (Wang et al., 2000). The $H_2S$ produced in the process reacts with dissolved metal ions, and the resulting insoluble metal sulfide is precipitated and removed from the solution (Graham et al., 2012; Kim et al., 2015; Hou et al., 2017; Xu et al., 2018). On the other hand, extracellular polymers (EPS) are used to adsorb heavy metal ions, and heavy metal ions are actively absorbed and transformed by intracellular metabolism and concentrated in the cell to reduce the harm of heavy metals (Wang et al., 2000; Chen et al., 2016). At the same time, the sulfate reduction process consumes hydronium ions in the water, increasing the pH value of the solution and precipitating heavy metal ions in the form of hydroxides (Gonzalez-Silva et al., 2009). This technology takes advantage of the differences in chemical properties of metal sulfates and sulfides(Ohfuji and Rickard, 2006; Zhou et al., 2013), as metal sulfates are highly soluble, but the corresponding metal sulfides have low solubility (Abdelouas et al., 2002; Kalwasinska et al., 2020).

Compared with microbial induced carbonate precipitation, SRB are more effective for removal of $Cd^{2+}$ and $Pb^{2+}$, and the sulfide solubility is much lower than that of carbonate minerals (Costa and Duarte, 2005; Wu et al., 2022). It also makes the microbial reduction of sulfate salt for remediation of heavy metal contamination a hot topic in the study of biomineralization. Based on the THIOPAQ system, a process was developed for sulfate reduction and oxidation of excess sulfides to remove heavy metals (Koschorreck et al., 2007). In this bioreactor, sulfate reducing bacteria used hydrogen as an electron donor to reduce sulfate to sulfide. Subsequently, sulfides were used to precipitate heavy metals, and excess sulfides were converted into elemental sulfur by sulfide oxidizing bacteria in the bioreactor; precipitated metal sulfides and elemental sulfur could also be reused(Zhang et al., 2004). studied the use of SRB to decontaminate a typical lead-zinc tailings reservoir in Yunnan Province. After microbial treatment, sampling and analysis showed that most of the heavy metals existed in the form of sulfides (Zheng et al., 2021). isolated and purified a new type of sulfate-reducing bacteria named *Pseudodesulfovibrio* from deep-sea cold springs. By studying the morphological characteristics, phylogenetic state and central metabolism of the strain, it was found that had strong tolerance to heavy metals and could immobilize of many kinds of heavy metal ions, such as $Co^{2+}$, $Ni^{2+}$, $Cd^{2+}$, $Hg^{2+}$ and so on (Zhao et al., 2021). Confirmed that SRB combined with different doses of nano-zero-valent Ion could treat cadmium-contaminated sediments. It was found that the content of free cadmium decreased and the content of stable cadmium increased, and cadmium was converted into sulfide precipitate by sulfate reduction.

In this study, the marine and freshwater sulfate-reducing bacteria *Desulfovibrio desulfuricans* and *Desulfobulbus propionicus* were selected, and the main objectives were as follows: (1) to compare the immobilization rate of *D. desulfuricans* and *D. propionicus* for heavy metals $Cd^{2+}$ and $Pb^{2+}$; (2) to clarify the process and mechanism of heavy metal mineralization mediated by microbial sulfate reduction. During the experiment, the changes of sulfate content, pH and Eh values during *D. desulfuricans* and *D. propionicus* growth in the presence of $Cd^{2+}$ and $Pb^{2+}$, and also to

determine their respective immobilization efficiencies of $Cd^{2+}$ and $Pb^{2+}$. The scanning electron microscope and energy dispersive spectroscopy (SEM-EDS), transmission electron microscope (TEM), X-ray diffractometer (XRD), Raman spectra and X-ray photoelectron spectroscopy (XPS) for solid phase characterization. Based on these researches, this study will provide a theoretical basis and new ideas for the application of sulfate reducing bacteria in heavy metal mine drainage remediation.

# 2 Materials and methods

## 2.1 Chemicals

Cysteine (purity≥ 99%); Anhydrous cadmium chloride ($CdCl_2$, analytical pure, purity≥99%); Lead nitrate ($Pb(NO)_3$, analytical pure, purity≥99%); Barium chloride ($BaCl_2{\cdot}2H_2O$, analytical pure, purity ≥99%).

## 2.2 Bacterium resource and cultivation

The marine sulfate-reducing bacteria, *Desulfovibrio desulfuricans* (ATCC 7757) was provided by BNCC Miner Biotechnology Collection, Beijing. The freshwater sulfate-reducing bacteria, *Desulfobulbus Propionicus* (ATCC 33891) was obtained from BioVector NTCC Inc., Beijing.

The proprietary culture medium used for *Desulfovibrio desulfuricans* is composed of the following: $KH_2PO_4$ 0.5 g, sodium lactate (70%) 4 g, $NH_4Cl$ 1.0 g, yeast extract 1.0 g, $CaCl_2{\cdot}6H_2O$ 0.1 g, $FeSO_4{\cdot}7H_2O$ 0.1 g, $Na_2SO_4$ 0.5 g, $MgSO_4{\cdot}7H_2O$ 0.2 g, distilled water 1,000 mL. The solid medium used for separation and purification was supplemented with 2% agar powder on the basis of Postgate C medium. Prior to culture, the medium was sterilized for 20 min at 121°C in an autoclave sterilization pot. Cysteine (100 mmol/L) was added to the liquid medium after sterilization through a sterile filter. The sulfate concentration in the medium was 1,000 mg/L.

*Desulfobulbus Propionicus* exclusive medium (2216E): yeast extract 1.0 g, peptone 5.0 g, beef extract 1.0 g, $FePO_4{\cdot}4H_2O$ 0.01 g, synthetic seawater 1,000 mL. Solid medium for separation and purification; add 2% agar powder to medium 2216E. Prior to culture, the medium was sterilized for 20 min at 121°C in autoclave sterilization pot. Cysteine 100 mmol/L was added to the liquid medium after sterilization through a sterile filter. The sulfate concentration in the medium was 1,000 mg/L.

## 2.3 Sulfate reduction and ORP test

Sulfate was used as the sulfur source for the experimental strains, and provided electrons for SRB during growth. The concentration of sulfate directly reflects the utilization capacity of the strain to sulfate, and provides the basis for reduction. The reducing ability of the strain can be verified by monitoring the concentration of sulfate during the growth process, and the barium sulfate turbidimetric method is used for this purpose. Firstly, the standard curve of sulfate was drawn: different volumes of sulphate standard solutions were aliquoted into 10 mL cuvettes in turn to obtain the final sulphate concentrations of 0, 50, 100, 150, 200 and 250 mg/L. The 2 mL of glycerol to ethanol solution and 1 mL 0.5 mol/L of hydrochloric acid solution were used. A 0.5 g of $BaCl_2{\cdot}2H_2O$ was added to each cuvette and mixed immediately. After standing for 15 min, the absorbance value of the sample was measured at 360 nm using a portable UV spectrophotometer (752 PC, JingHua Instruments). The concentration of sulphate of the sample was measured in units of mg/L; the absorbance in ABS was measured each time and a standard sulphate curve was plotted. The sampling intervals were at 0, 12, 24, 48, 72, 96, 120 and 144 h. Three replicates were made for each test sample. One milliliter of each sample was centrifuged at 4,000 r/min for 10 min and then passed through a 0.22 μm disposable sterile filter membrane and diluted in a 10 mL colorimetric tube for measurement.

For determination the ORP (Oxidation-Reduction Potential) value during the incubation, using a precision pH meter to replace the ORP special measurement electrode, 5 mL of bacterial liquid was taken and tested.

## 2.4 Heavy metal mineralization test

The rates of heavy metal immobilization by *D. desulfuricans* and *D. propionicus* were tested at different initial concentrations of $Cd^{2+}$ and $Pb^{2+}$. The 0.2 mL of prepared bacterial suspension were added to anaerobic bottles containing 200 mL of $Cd^{2+}$ solution (0, 10, 20, 30, 50, 100 mg/L) and 200 mL of $Pb^{2+}$ solution (0, 10, 30, 50, 80, 150 mg/L), respectively. The control group was inoculated into medium with an equal amount of sterile water, and the three groups were prepared and cultured under an anaerobic condition. The samples were incubated at 30°C and 150 r/min. The culture solution was then centrifuged and filtered, and the supernatant was used to determine the concentrations of $Cd^{2+}$ and $Pb^{2+}$, the precipitated fraction was collected to characterize heavy metal mineralization.

## 2.5 Determination of $Cd^{2+}$ and $Pb^{2+}$

Before each sampling, the serum bottle was thoroughly shaken, and aliquots of 5 mL samples for total metal concentration were taken from the cultures at 0, 12, 24, 48, 72, 96, 120 and 144 h consecutively, centrifuged at 8,000 r/min for 10 min and then passed twice through 0.22 μm disposable sterile filter membranes. Each experiment was performed in triplicate. Supernatant acidified using ultra pure $HNO_3$ (5% v/v) and stored at 4°C until analyzed by ICP-MS (X SERIES II, Thermo Fisher Scientific).

## 2.6 Characterization of the cells and biologically mineralized precipitates

After the reduction experiment, the morphology and structure of the bacteria and mineralized precipitates were observed with a SEM (Hitachi S-4800, Japan), TEM (Hitachi H-7650, Japan) and EDS (Hitachi S-4800, Japan). In order to acquire high quality SEM and TEM images, bacterial samples were collected by centrifugation (4,000 r/min, for 10 min), fixed with 2.5% glutaraldehyde and

washed two times with 0.1 mol/L phosphate buffered saline (PBS). Afterwards, the cells were gradually dehydrated with successive 30%, 50%, 70%, 80% and 100% ethanol treatments for 20 min, followed by a treatment with acetone. Finally, the samples were dried with a $CO_2$ critical point desiccator for 10 h for morphological analysis.

The mineralized precipitates were collected by centrifugation (10,000 r/min,10 min), washed three times with ultrapure water, frozen at −80°C for 2–4 h, and then freeze-dried in a vacuum freeze dryer and stored at −20°C for further analysis.

XRD (Bruker D8 Focus Powder XRD) of precipitates used a Cu Kα ray for detection. The parameters were set at 36 kV and 20 mA, the scanning angle was set at 10°–70°, the step size and scanning speed were 0.02°and 0.5°(2θ)/min, respectively.

Raman spectra of mineralized precipitates were conducted with a Renishaw Micro-Raman Spectrometer (Renishaw in Via Reflex) using 532 nm laser excitation with wavenumber range of 100–1,200 $cm^{-1}$.

XPS (Thermo ESCALAB 250 XI, USA) spectra of mineralized precipitates were carried out by using a monochromatic AI Ka X-ray source (hv = 1,486.6 eV) at 150 W, and an X-ray beam spot of 500 μm. The survey spectra were collected at fixed analyzer pass energies of 30 eV.

## 2.7 Statistical analysis

All experimental data are the means of three parallel experiments, indicated as means ± standard error. Origin 9.1 software is used for data processing and mapping, MDI Jade 6 software is used for XRD analysis, and ANOVA was then applied for statistical analysis of the results to interpret the significance of these metals immobilization rate as well as on sulfate removal in the study.

Equation 1 is calculating the sulfate reduction rate and Cd and Pb immobilization rate:

$$R(\%) = (C_0 - C_t)/C_0 \times 100\% \quad (1)$$

where $R$ is the sulfate reduction rate or immobilization rate of $Cd^{2+}$ and $Pb^{2+}$, %; $C_0$ is the concentration of $SO_4^{2-}$, $Cd^{2+}$ and $Pb^{2+}$ in control group, mg/L; $C_t$ is the concentration of $SO_4^{2-}$, $Cd^{2+}$ and $Pb^{2+}$ in the experimental group, mg/L.

# 3 Results and discussion

## 3.1 *D. desulfuricans* and *D. propionicus* growth characteristics and sulfate reduction capacity in the presence of $Cd^{2+}$ and $Pb^{2+}$

With the initial sulfate concentration of 1,000 mg/L and incubation temperature at 30°C, *D. desulfuricans* grew rapidly, entering the logarithmic growth phase in about 12 h (Supplementary Figure S1A). The strains entered a stable period at 48 h, and after 60 h the growth was significantly delayed, which might be due to the toxic effect of $H_2S$ produced by the metabolism of sulfur-reducing bacteria under fully closed conditions, inhibiting the growth of the microorganism. Meanwhile, the sulfate concentration gradually decreased, and at 144 h of incubation the sulfate concentration was 340 mg/L, and the sulfate reduction rate reached 66% (Supplementary Figure S1A). When the initial sulfate concentration was set to 4,000 mg/L, the growth of *D. propionicus* was relatively slow compared to *D. desulfuricans*, lagging behind the logarithmic phase, and entering the relatively weak growth period into the stationary growth phase at 72 h (Supplementary Figure S1B). After 144 h of incubation, the sulfate concentration was reduced to 1860 mg/L, and the sulfate reduction rate by *D. propionicus* reached 53% (Supplementary Figure S1B). *D. propionicus* was more suitable for high concentration of sulfate than *D. desulfuricans*, and they had a strong ability for sulfate reduction.

The initial concentration of sulfate affected the growth and activity of microorganisms, and the ability of sulfate-reducing bacteria to immobilize heavy metal ions could be gauged according to their tolerance and their ability to reduce sulfate. The sulfate reduction abilities of the two bacteria grown in the presence of $Cd^{2+}$ and $Pb^{2+}$ and with different initial concentrations of sulfate were shown in the Figure 1. In terms of heavy metals, it could be seen that $Cd^{2+}$ had a greater influence on growth activity and sulfate reducing ability of sulfate-reducing bacteria than that of $Pb^{2+}$, and the two bacteria still had good sulfate reducing ability in the presence of heavy metals (Figures 1a–d). The freshwater sulfate-reducing bacteria *D. propionicus* had an obvious advantage over the marine sulfate-reducing bacteria *D. desulfuricans* in tolerance to sulfate, and also in the reduction of sulfate with increased time.

Taking the addition of 10 mg/L $Cd^{2+}$ as an example, it could be seen from the Figure 1a that the low concentration of sulfate promoted growth and reduction capacity of *D. desulfuricans*, but when the initial sulfate concentration exceeded 1,100 mg/L, the ability to reduce sulfate was obviously impaired. Sulfate reduction rate of *D. desulfuricans* declined to 51.42% over 48 h when the initial concentration of sulfate was 1,100 mg/L. The $H_2S$ might be generated in the process of sulfate reduction, which was a harmful gas with toxic effects on bacteria in a completely anaerobic closed environment, and could reduce the activity of *D. desulfuricans*. When the initial concentration of sulfate was 1,300 mg/L, only 17.93% of the sulfate was reduced in about 24 h, thereafter the reduction rate slowly reached about 34% after 96 h. Sulfate reduction rate of *D. desulfuricans* was greatly affected by the initial sulfate concentration; however, when the initial concentration of sulfate exceeded 1,500 mg/L, the bacteria in the solution were obviously affected by higher sulfate concentration, and the bacteria did not increase in numbers. Therefore, the activity was greatly reduced, and there was little or no sulfate reduction.

*D. propionicus* under 10 mg/L $Cd^{2+}$ and an initial sulfate concentration of 4,000 mg/L achieved a sulfate reduction rate of 46.23% after 144 h and still showed an increasing tendency; however, it had already reached the optimal sulfate concentration. When the initial concentration of sulfate was adjusted to 9,000 mg/L, the reduction rate of the bacteria to sulfate still reached 8.12% at 144 h (Figure 1b). *D. propionicus* had a greater tolerance to high sulfate concentrations and a greater reduction capacity at these levels than *D. desulfuricans*.

The ORP value is an important parameter in the process of reactive hydrolysis, and it is the main basis for comparing the activity of sulfate-reducing bacteria (Kurdowski and Bochenek,

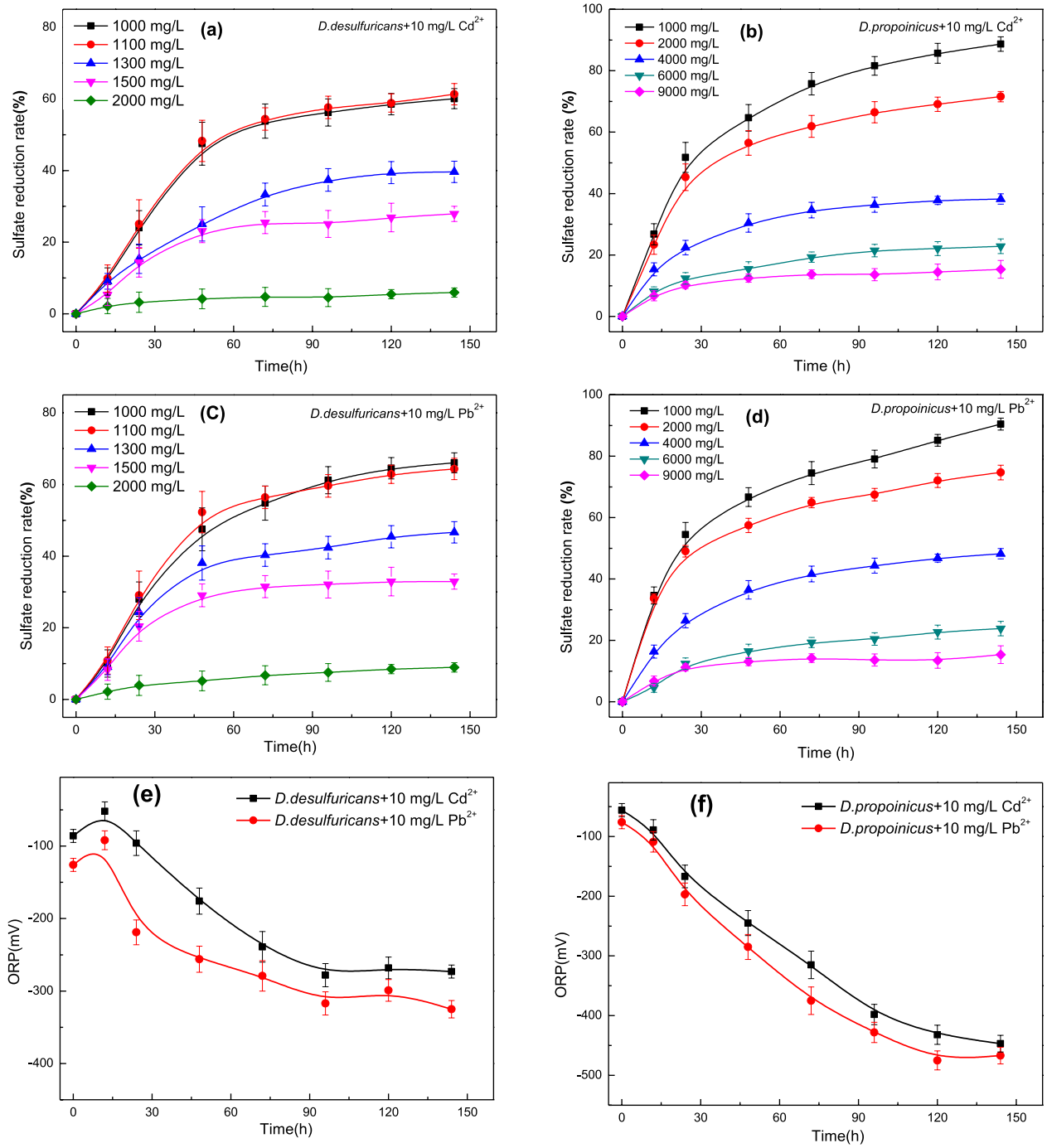


FIGURE 1
Effects of initial $SO_4^{2-}$ concentration on sulfate reduction and changes in ORP value by *D. desulfuricans* **(a, c, e)** and *D. propionicus* **(b, d, f)** in the presence of $Cd^{2+}$ and $Pb^{2+}$.

2012). Redox potentials are correlated with cell density and biological activity in biofilms. The growth of sulfate reducing bacteria uses sulfate as the final electron acceptor (Dickinson et al., 1997). However, from a chemical point of view, sulfate is not a favorable electron acceptor for microorganisms because the redox potential of $S^{2-}$ is about −516 mV (Parshina et al., 2005; Ashraf et al., 2019), which is too low for microbial growth. But the metabolic processes within sulfate-reducing bacteria can enhance the process of reduction through depolarization of hydrogen, sulfide production and the formation of a surface consisting of a semi-conductive iron sulfide film (Qian et al., 2015; Alam and McPhedran, 2019). For the microbial sulfate reduction systems, the biochemical reactions that occur during sulfate reduction in the cell will lead to changes in ORP.

Changes in the ORP value for the reaction stage of sulfate reduction by *D. desulfuricans* and *D. propionicus* after adding 10 mg/L $Cd^{2+}$ indicated metabolic changes in the system. As

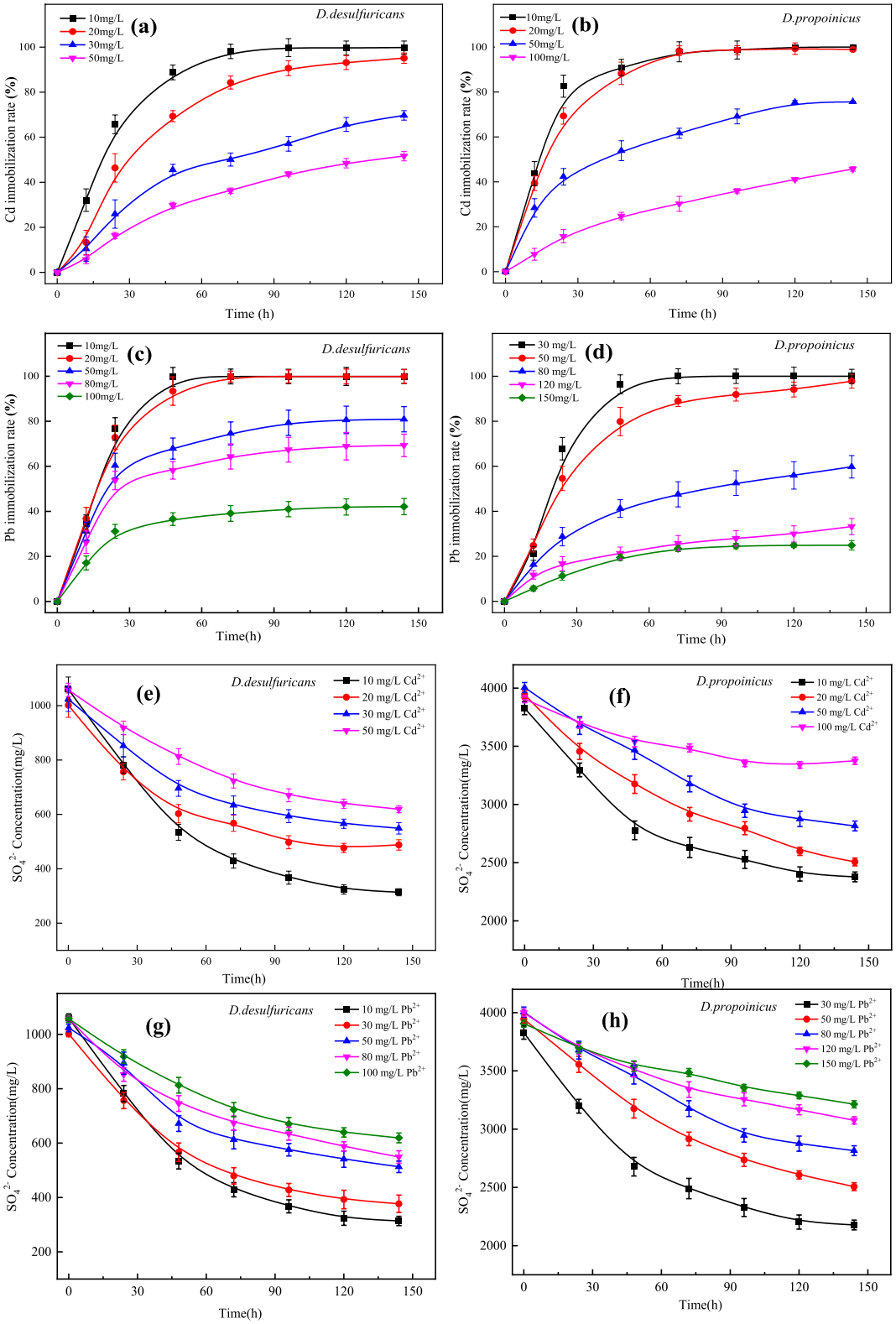


FIGURE 2
Heavy metal immobilization rates and sulfate concentrations for *D. desulfuricans* **(a, c, e, g)** and *D. propionicus* **(b, d, f, h)** at different initial concentrations of $Cd^{2+}$ and $Pb^{2+}$.

shown in Figure 1e, during the sulfate reduction process of *D. desulfuricans*, a temporary increase of ORP occurred in the early stage of the reaction. Due to the hydrolysis of $CO_3^{2-}$ and the combination of $H^+$ and $CO_3^{2-}$, the ORP value increased. Subsequently, a large number of metabolites were produced, with $S^{2-}$ being the main metabolite in the form of $H_2S$; this led to a rapid decrease in the ORP value of the system through the toxicity of $H_2S$.

The ORP value in medium with *D. propionicus* might be influenced by high concentration of sulfate over a short period; the process leading to an increase in ORP was not obvious, though the reduction reaction was strong and the overall trend in ORP was declining (Figure 1f). However, the reduction reaction of both bacteria gradually tended to stabilize after 100 h in general. These changes might be related to the growth, metabolic activities and biofilm development. Sulfate reducing bacteria formed biofilms during sulfate reduction, and the metabolic activities of microorganisms might be affected by the production of sulfide, the formation of iron sulfide, and the formation of extracellular polymers; these together, improved the reduction speed and quality of the microbial system.

## 3.2 Mineralization of $Cd^{2+}$ and $Pb^{2+}$ and sulfate reduction by *D. desulfuricans* and *D. propionicus*

Mineralization of $Cd^{2+}$ by *D. desulfuricans* and *D. propionicus* was shown in the Figures 2a, b. When the concentration of $Cd^{2+}$ was at 10 mg/L for about 72 h, the immobilization efficiency of *D. desulfuricans* for $Cd^{2+}$ reached 98.9%, after which it would become stable. With increased $Cd^{2+}$ concentration, the growth of *D. desulfuricans* was suppressed, and there was a corresponding reduction in immobilization rate of $Cd^{2+}$. The totals of $Cd^{2+}$ mineralized were 95.1%, 65.7% and 51.6% at concentrations of 20, 30 and 50 mg/L $Cd^{2+}$ over 144 h respectively. It could be seen that the removal rates of $Cd^{2+}$ were closely related to their growth curves. *D. propionicus* had a stronger tolerance to $Cd^{2+}$ and a greater mineralization effect on $Cd^{2+}$ than *D. desulfuricans*, whose immobilization rate could reach 77% over 144 h when the initial concentration of $Cd^{2+}$ was 50 mg/L. That was to say, *D. propionicus* had a very good mineralization effect on heavy metals when the growth environment met the basic requirements.

Mineralization of $Pb^{2+}$ by *D. desulfuricans* and *D. propionicus* was shown in Figures 2c, d. *D. propionicus* had achieved 80% immobilization efficiency of $Pb^{2+}$ after 48 h with an initial $Pb^{2+}$ concentration less than 50 mg/L, and the final amount of $Pb^{2+}$ mineralized was 98%. The sensitivity of the strain to the presence of $Pb^{2+}$ was lower than that to $Cd^{2+}$, but the immobilization rate decreased with increased $Pb^{2+}$ concentration. When the concentrations of $Pb^{2+}$ were 80, 120 and 150 mg/L, the maximum amounts of $Pb^{2+}$ mineralized over 144 h were 57.1%, 28.2% and 19.7%, respectively. It could be seen that the immobilization rate of $Pb^{2+}$ was closely related to its growth activity.

In this study, sulfate reduction rate of *D. desulfuricans* and *D. propionicus* were reduced with the increase of heavy metal ion concentration (Figures 2e–h), this might be because the toxicity of heavy metal ions would affect the growth activity of microorganisms, at the same time, heavy metal ions for microbial biofilm and enzyme activity damage could also affect the metabolic pathway of sulfur reducing bacteria, thus reducing the reduction rate of sulfate. However, microorganisms possess physiological and chemical resistance mechanisms to counteract the toxicity of heavy metal ions in their environment (Yin et al., 2019; Zhuang et al., 2024) have suggested that the bacteria might increase gene expression to compensate for the declining bacterial count and maintain sulfate reduction rates. As a result, even at high concentrations of $Cd^{2+}$ and $Pb^{2+}$, both strains of SRB retain their sulfate-reducing capability, albeit at a reduced rate.

*Desulfovibrio desulfuricans* and *Desulfobulbus propionicus* are typical functional bacterial species that can transform $SO_4^{2-}$ to sulfide by acting as the terminal electron acceptor in the process of dissimilatory sulfate reduction, in which the sulfate concentration is gradually decreasing, as shown in Supplementary Figure S1. In this process, the metabolic pathway of sulfate reduction in SRB initiates with the enzyme sulfate adenosine transferase (Sat), which facilitates the active transport of $SO_4^{2-}$ across the plasma membrane (Hu et al., 2024). This action results in the generation of adenosine phosphosulfate (APS) and pyrophosphate (PPi). APS is subsequently reduced to $SO_3^{2-}$ under the catalysis of APS reductase. Further reduction of sulfite to $H_2S$ is accelerated by the enzyme acidic sulfite reductase (CBS). The culminating step involves the reaction of sulfide $S^{2-}$ with various heavy metal ions, including $Cd^{2+}$ and $Pb^{2+}$, leading to the formation of stable metal sulfides. This process effectively immobilizes the heavy metals, rendering them less bioavailable and toxic (Hu et al., 2024).

## 3.3 Effect of initial pH on mineralization of $Cd^{2+}$ and $Pb^{2+}$ by *D. desulfuricans* and *D. Propionicus*

In order to further study the optimal pH conditions for metal mineralization by the two sulfate-reducing bacteria in the presence of heavy metals $Cd^{2+}$ and $Pb^{2+}$, the initial pH gradients of the culture media were set as 5.0, 6.0, 7.0, 8.0 and 9.0, respectively. The results of Figures 3a, b showed that *D. desulfuricans* mineralized $Cd^{2+}$ and $Pb^{2+}$ at an optimal pH of 7.0, and the metal mineralization capacity of *D. desulfuricans* at pH 6.0 and pH 9.0 decreased markedly relative to the mineralization capacity at the optimal pH, but there were no differences between these two pH values. However, when the pH was set to 5.0, the immobilization rate of $Cd^{2+}$ and $Pb^{2+}$ by *D. desulfuricans* had decreased to 27.98% and 47.12% over 144 h, respectively. Thus, the pH value had a great influence on the growth and activity of *D. desulfuricans*; low pH values likely affected the enzymatic activity driving metabolic processes, and ultimately, the ability to mineralize heavy metals.

*D. propionicus* had an optimal pH of about 8.0 for heavy metal mineralization in the presence of $Cd^{2+}$ and $Pb^{2+}$ (Figures 3c, d). *D. propionicus* showed greater adaptability to a weak alkaline environment than did *D. desulfuricans*. The growth activity of *D. propionicus* was suppressed to a certain extent under alkaline conditions, though it still showed good immobilization rates; thus, it was demonstrated that *D. desulfuricans* had good environmental adaptivity.

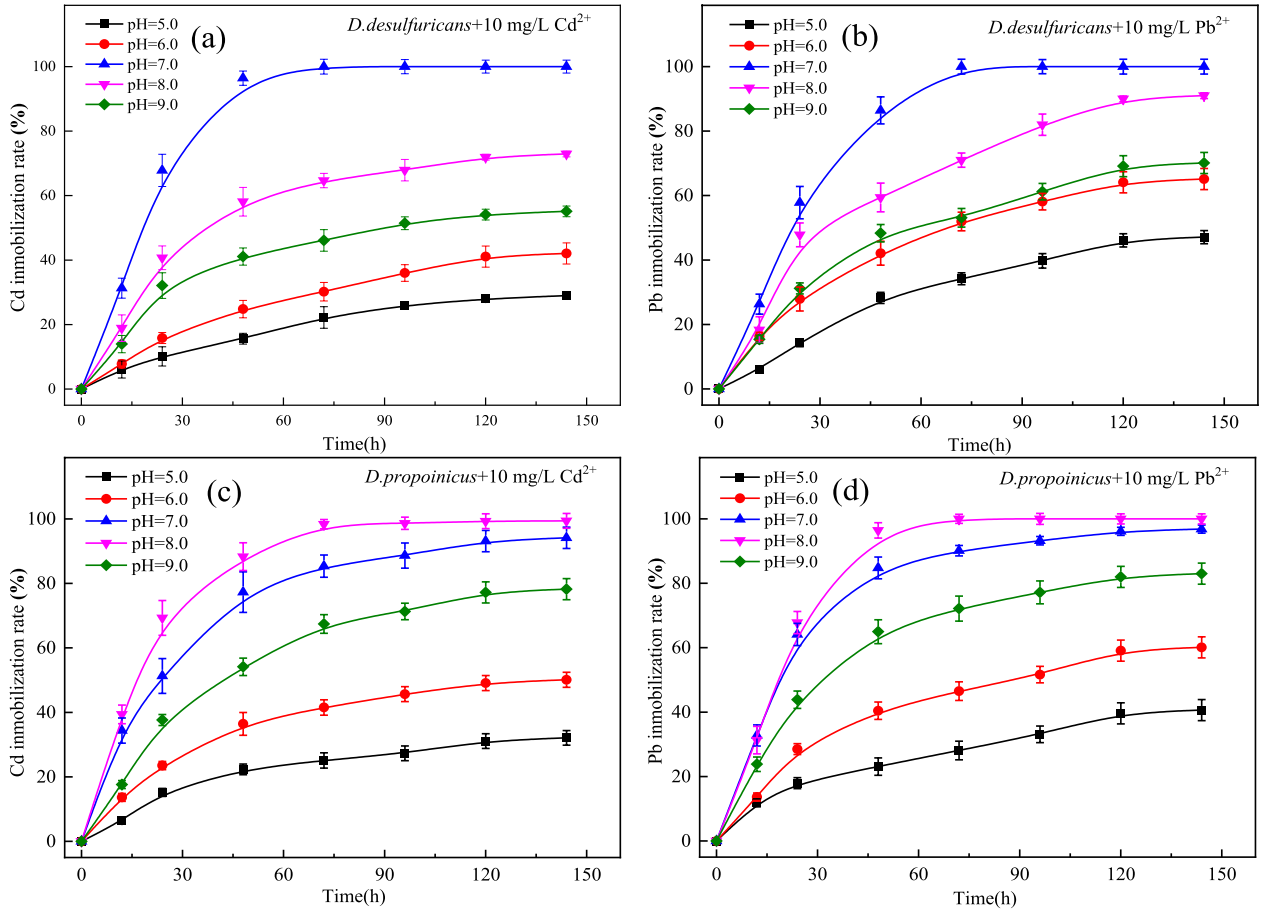


FIGURE 3
Effect of initial pH on immobilization of $Cd^{2+}$ and $Pb^{2+}$ by *D. desulfuricans* **(a, b)** and *D. propionicus* **(c, d)**.

## 3.4 SEM images and EDS analysis of the mineralized precipitate

In order to clarify the characteristics of heavy metal precipitation produced by *D. desulfuricans* and *D. propionicus*, the precipitates were collected and analyzed. Through observation of the surface morphology of the bacteria with SEM, it could be seen that *D. desulfuricans* was initially cylindrical, smooth in outline and smooth in edge. After the cultivation with 10 mg/L $Cd^{2+}$ for 144 h, precipitates began to adsorb on the surface of the bacterial cell wall, which also reflected its immobilization effect on heavy metals (Figure 4a). This indicated that Cd had a certain toxic effect on the growth and activity of *D. desulfuricans*. Obvious shrinkage and depression of the thallus was accompanied by widened and broken holes. Figure 4b showed that after the cultivation with 10 mg/L $Pb^{2+}$, precipitation increased significantly around the bacterial cell, which might be related to the thallus gradually becoming alkaline to form lead oxides and hydroxides in the microorganism growth process.

Figure 4c showed that the bacteria *D. propionicus* were flat and highly irregular and formed unique lobes. After *D. propionicus* had been cultured with 10 mg/L $Cd^{2+}$ for 144 h, the volume of *D. propionicus* cells were reduced and obvious shrinkage had occurred. The surface structures of the precipitates were dense and mostly showed irregular spherical structures, which were adsorbed and accumulated on the surfaces of the cells.4d showed that *D. propionicus* cultured with 10 mg/L $Pb^{2+}$ for 144 h had more complex precipitates, which were more diversified in structure. The precipitates were loose and porous, and covered the entire bacterium.

EDS analysis also showed that the elements in the precipitates induced by sulfate-reducing bacteria contained C, O, S, Cd and C, O, S, Pb, which further indicated that heavy metal ions $Cd^{2+}$ and $Pb^{2+}$ had been adsorbed and mineralized by these two sulfate-reducing bacteria *D. desulfuricans* and *D. propionicus*. Research has been reported that SRB possess genes for sulfate reduction, including ATP sulfurylase (*sat*), APS reductase (*aprA* and *aprB*), and dissimilatory sulfite reductase (*dsrAB* and *dsrC*) (Venceslau et al., 2011; Zhong et al., 2024a). Previous study has showed that the upregulation of *sat* and *aprA* genes of bacteria might enhance assimilatory sulfate reduction to resist heavy metal ions (such as $Cd^{2+}$) toxicity (Zhang et al., 2023). Such gene expression could ensure its own growth by enhancing the sulfate metabolism. Besides, the upregulation of *sat* and *aprA* gene expression with the addition of metal ion reflected the SRB response to complex survival environment (Zhong et al., 2024b; Zhuang et al., 2024). This is sufficient to explain why, despite the increase in $Cd^{2+}$ and $Pb^{2+}$ concentrations, *D. desulfuricans* and *D. propionicus* still retained a certain sulfate conversion capacity and ultimately

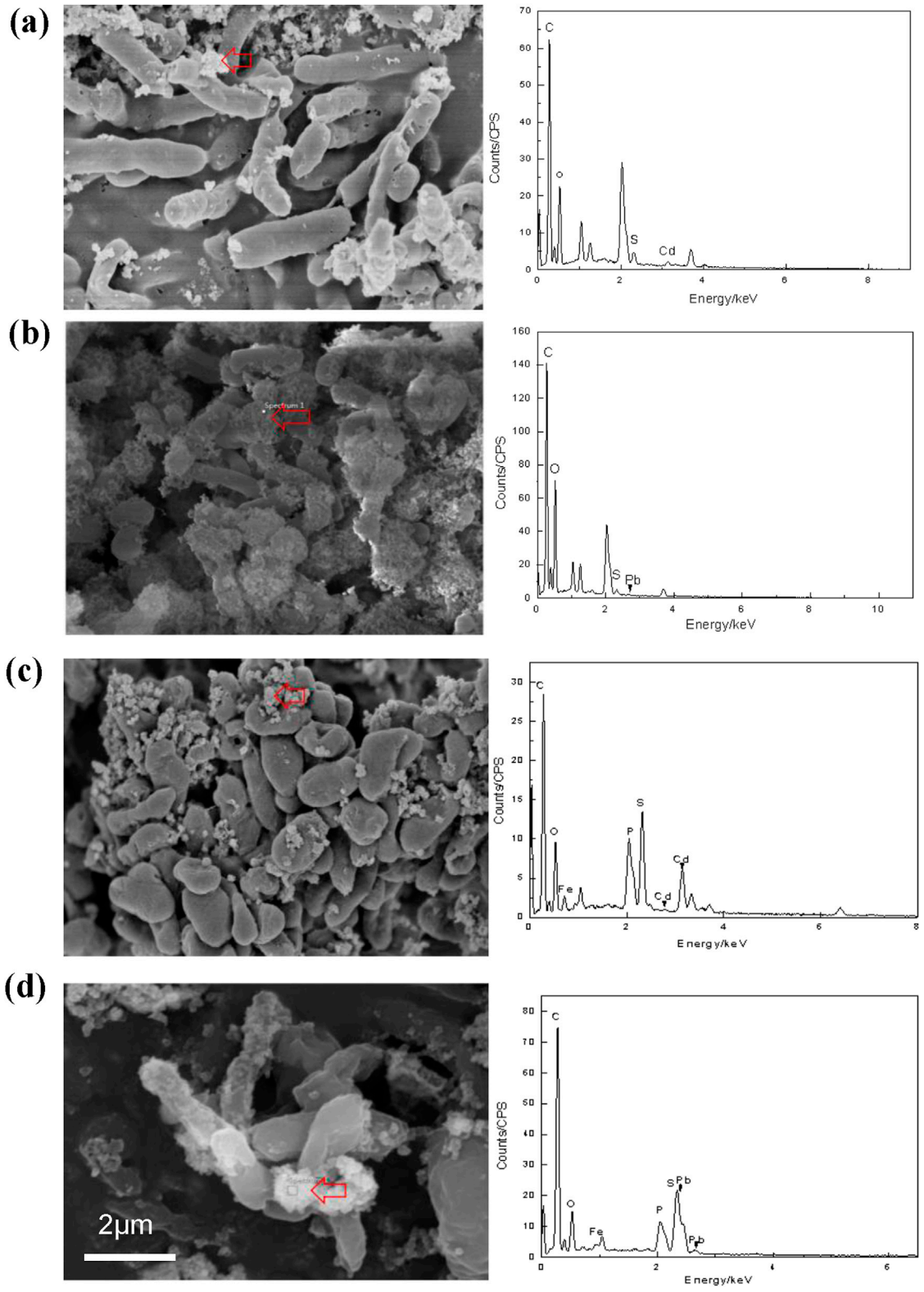


FIGURE 4
SEM images of *D. desulfuricans* **(a, b)** and *D. propionicus* **(c, d)** exposed to10 mg/L $Cd^{2+}$ and $Pb^{2+}$ for 144 h. Red arrows indicated the mineralized precipitate outside the bacterial cells. EDS analysis of the mineralized precipitates were shown at the locations of the arrows in the pictures. Scale bars: **(a–d)** 1 μm.

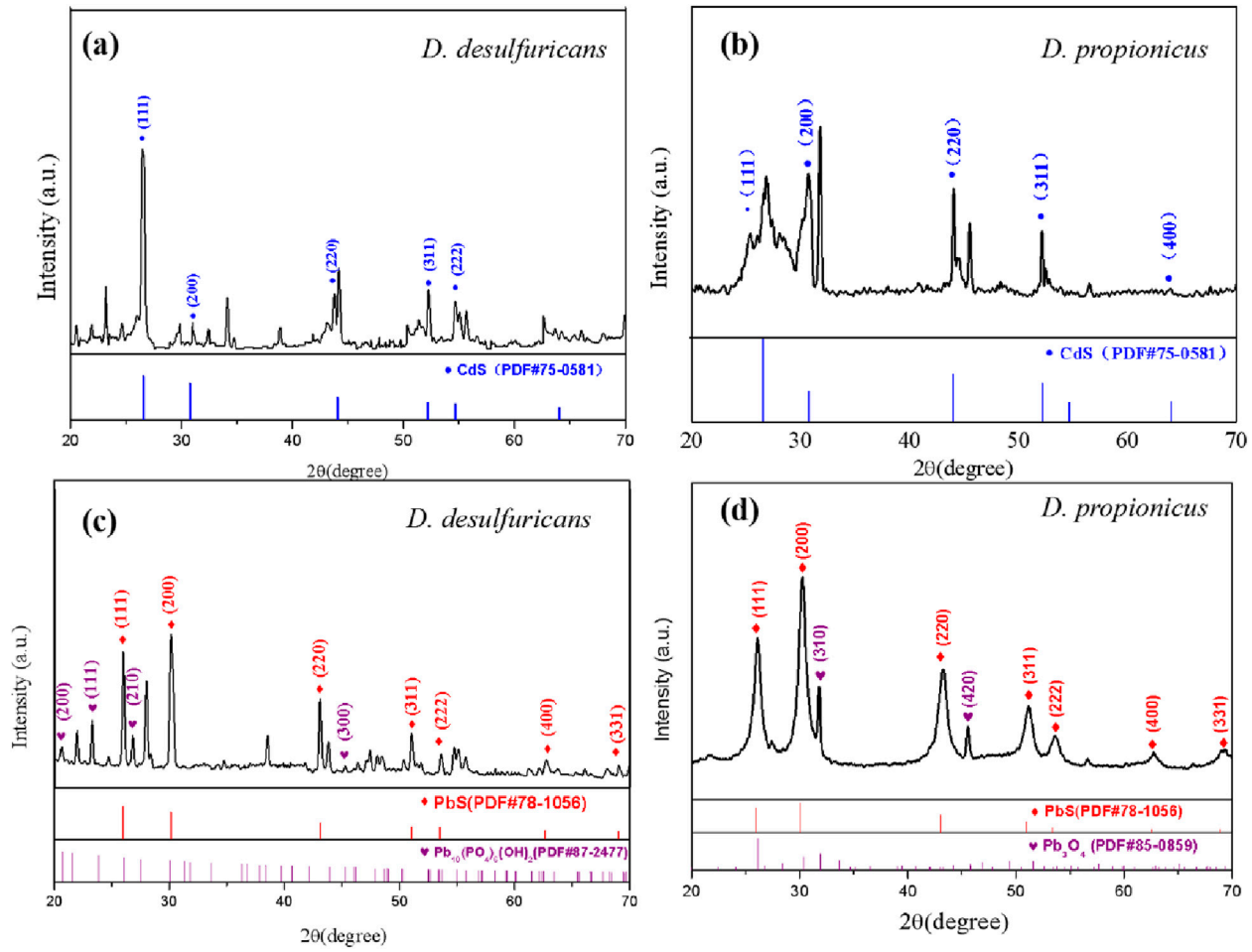


FIGURE 5
The XRD pattern of mineralized precipitates formed by *D. desulfuricans* **(a, c)** and *D. propionicus* **(b, d)** after 144 h incubation in medium containing 10 mg/L $Cd^{2+}$ and $Pb^{2+}$, respectively.

immobilized the $Cd^{2+}$ and $Pb^{2+}$ as insoluble precipitates on the bacterial surface.

Representative unstained whole-mount transmission electron micrographs of *D. desulfuricans* observed at 144 h showed a consistent morphology associated with mineralized heavy metals that was observed throughout the time course experiment. Combined with EDS, it was tentatively determined to be a loose, fine-grained FeS precipitate, and it could be seen from the TEM images that the addition of metal ions had a certain impact on the growth of these microorganisms. There were black and gray particles embedded and attached in a circle on the surface of bacteria, which were unevenly distributed on the surface of the thallus (Supplementary Figure S2). When *D. desulfuricans* was cultured with 10 mg/L $Pb^{2+}$ for 144 h, the sediment around *D. desulfuricans* became more obvious and was accompanied by flaky material. Combined with XRD, it seemed that the material might be a compound created in the process of bacterial phosphorylation. These results indicated that $Cd^{2+}$ and $Pb^{2+}$ had certain toxic effects on the growth of these microorganisms, and the process of $Cd^{2+}$ and $Pb^{2+}$ mineralized by sulfate-reducing bacteria was mainly carried out on the bacterial surface.

## 3.5 XRD analysis of the mineralized precipitate

Figures 5a,b showed the XRD pattern of mineralized precipitate generated by culturing *D. desulfuricans* with 10 mg/L $Cd^{2+}$ for 144 h. According to the JADE6 peak search, diffraction peaks appeared at 2θ values of 26.7°, 30.9°, 44.1°, 52.4° and 54.8°. After JADE6 retrieval, the XRD pattern was found to be consistent with the positions and intensities for the characteristic peaks of the face-centered cubic CdS structure (PDF#75–0581) standard card. The crystal plane index of the corresponding CdS was (111), (200), (220), (311) and (222). Figure 5c showed the XRD pattern of mineralized precipitate generated by culturing *D. desulfuricans* with 10 mg/L $Pb^{2+}$ for 144 h. The diffraction peaks appeared at 2θ values of 26.1°, 30.2°, 43.1°, 51.2° and 53.6°, which was consistent with the positions and intensities for the characteristic peaks of the face-centered cubic PbS structure (PDF#78–1,056). Additionally, the diffraction peaks appeared at 2θ values of 20.6°, 23.3°, 26.7°, and 45.3°, which was related to $Pb_{10}(PO_4)_6(OH)_2$ (PDF#87–2477). Combined with the XRD analysis results, this confirmed that CdS and PbS existed in the precipitates, and *D. desulfuricans* had a significant mineralization effect on Cd and Pb.

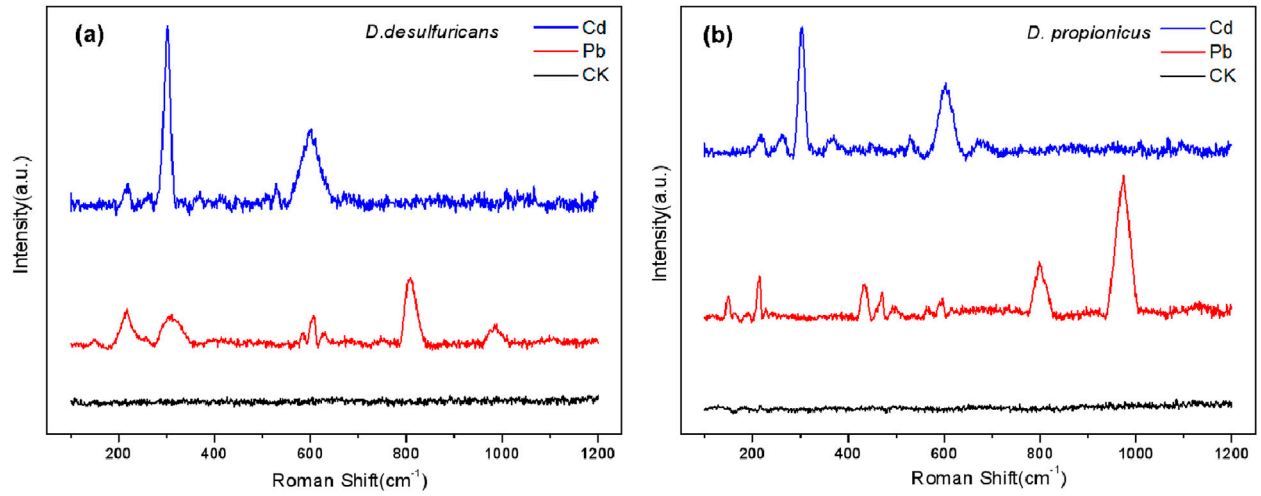


FIGURE 6
The Raman scattering spectra acquired for the mineralized precipitates formed by *D. desulfuricans* **(a)** and *D. propionicus* **(b)**.

Figure 5d showed the XRD pattern of precipitate generated by culturing *D. propionicus* with 10 mg/L $Pb^{2+}$ for 144 h. The diffraction peaks appeared at 2θ at 26.0°, 30.1°, 35.2°, 51.2°, 53.6°, 62.8° and 69.1°, which was consistent with the characteristic peaks of PbS structure (PDF#78–1,056). Additionally, the diffraction peaks appeared at 31.8° and 45.6° at 2θ, which was related to $Pb_3O_4$ (PDF#85–0859), and the crystal plane index of $Pb_3O_4$ was (310) and (420). This demonstrated that the mineralized precipitates of *D. propionicus* cultured in the presence of lead ions were mainly PbS and $Pb_3O_4$, which was also in accordance with the EDS data.

SRB is able to utilize sulfate as the terminal electron acceptor for the metabolism of organic substrates under anaerobic condition, and sulfate is transformed to sulfide which can stably precipitate with $Cd^{2+}$ and $Pb^{2+}$, which were the main product in biomineralization system. This process can be expressed by Equations 2–5 (Hu et al., 2024). The insoluble metal sulfides exhibit remarkably low solubility, excellent sedimentation properties, and low bioavailability. Besides, according to Figures 5c,d, $Pb_{10}(PO_4)_6(OH)_2$ and $Pb_3O_4$ were discovered in samples. This observation might be due to the fact that microbial sulfate reduction would cause electron transfer phosphorylation (Sievert and Kuever, 2000; Song et al., 2019). Phosphate was one of the important functional groups on the cell surface, involved in the interaction of lead ions with cells, to precipitate the lead ions combined with the sulfur ions (Belyakova et al., 2006; Cardenas et al., 2010; Li et al., 2021). This also could be seen in EDS analysis, showing that elemental phosphorus was involved in the formation of some of the mineralized precipitate. When *D. desulfuricans* strain was used to fix lead ions, the precipitation product was $Pb_{10}(PO_4)_6(OH)_2$. For *D. propionicus* cultivation, $Pb_3O_4$ and $PbSO_4$ were also present in the precipitation products because of the high sulfate concentration in the culture conditions (Parshina et al., 2005; Mallhi et al., 2019).

$$AMP^{4-} + SO_4^{2-} + H^+ \rightarrow APS^{2-} + HP_2O_7^{3-} \quad (2)$$

$$APS^{2-} + 2e^{2-} + H^+ \rightarrow HSO_3^- + AMP^{2-} \quad (3)$$

$$HSO_3^- + 6e^{2-} + 6H^+ \rightarrow HS^- + H_2O \quad (4)$$

$$H_2S + M^{2+} \rightarrow 2H^+ + MS \quad (5)$$

It was also noted that *D. desulfuricans* had a relatively high number of spurious peaks from comparison of the XRD patterns of the two species; this might have resulted from the formation of secondary minerals of iron oxide and Cd-S-Fe type due to a small amount of Fe in the culture medium, which was consistent with the research conclusion of (Zhao et al., 2021). Comparatively, mineralized metal precipitate of *D. propionicus* had a more stable crystal structure and relatively fewer stray peaks.

## 3.6 Raman characterization of the mineralized precipitate

As could be seen in Figures 6a, b, the main peaks of the Raman spectra of the precipitates obtained after culture in medium containing $Cd^{2+}$ were located at 303 and 606 $cm^{-1}$, which could be regarded as the first and second order longitudinal optical vibration modes of CdS respectively (Xu L. et al., 2021). After culture in medium containing $Pb^{2+}$, signal changes could be seen at 309 and 812 $cm^{-1}$. By referring to the spectrogram, it could be seen that these peaks were related to Pb oxide, while the main peak at 974 $cm^{-1}$ in Figure 6b was consistent with $PbSO_4$. That might be because *D. propionicus* was more tolerant of high sulfate concentrations and the precipitate from *D. propionicus* was a good match for lead sulfate.

On the other hand, extracellular polymer (EPS) also adsorbed heavy metal ions. FTIR data analysis showed that cell surface functional groups such as carboxyl group, group and phosphate group might participate in the adsorption of metal ions (Supplementary Figure S3). Through their own metabolism, cells actively absorbed and transformed heavy metal ions and enriched them in the body, reducing the harm of heavy metals.

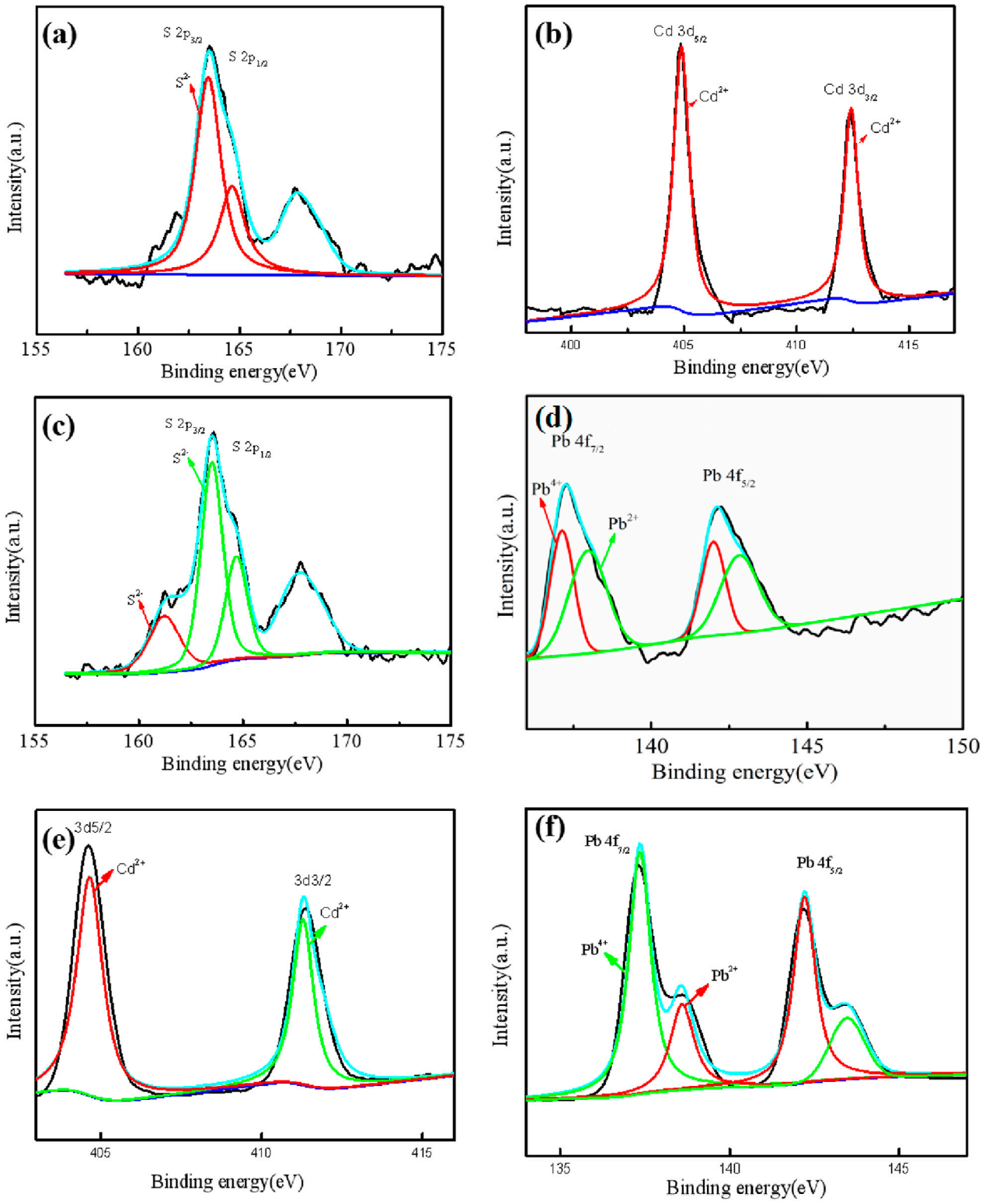


FIGURE 7
The XPS spectra of the mineralized precipitates formed by *D. desulfuricans* **(a–d)** and *D. propionicus* **(e, f)**. The high-resolution spectra of Cd3d **(b)** and Pb4f **(d)** and corresponding orbitals S2p **(a, c)** for *D. desulfuricans*. The high-resolution spectra of Cd3d **(e)** and Pb4f **(f)** for *D. propionicus*.

### 3.7 XPS analysis of the mineralized precipitate

Figure 7a showed the XPS analysis of the precipitate after 144 h of *D. desulfuricans* culture in containing 10 mg/L $Cd^{2+}$ medium. Four different characteristic peaks appeared after the S2p track, and sorted between 161 and 172 eV (Figure 7c). According to the XPS standard spectrum, the peaks appeared at 163.10 and 164.93 eV corresponding to 2p3/2 orbit of $S^{2-}$. Figure 7b was the characteristic peak of *D. desulfuricans* cultured with $Cd^{2+}$. Two characteristic peaks appeared after the Cd3p track, splitting between 403 and 415 eV. According to the XPS standard spectrum, $Cd^{2+}$ peaked at 3d5/2 and 3D3/2, and correspond to 405.10 and 412.00 eV, respectively; the 405.10 eV radiation corresponded to the Cd-S bond formed by the mineralization of $Cd^{2+}$. Figure 7f showed the XPS analysis spectrum of the precipitate after 144 h of *D. propionicus* mineralizing $Pb^{2+}$. Four characteristic peaks appeared after the Pb4f track, separating between 135 and 146 eV. It could be seen from the XPS standard spectrum that the peaks of $Pb^{4+}$ at 4f7/2 and 4f5/2 corresponded to 137.48 and 142.20 eV respectively, which might be the combination of O in the reduction process to form $PbO_2$ and $Pb_3O_4$. The peak of $Pb^{2+}$ at 4f7/2 and 4f5/2 corresponded to 138.55 and 143.45 eV, respectively, and also corresponded to the Pb-S bond formed by the mineralization of $Pb^{2+}$. In brief, the treated samples were composed of CdS and PbS, which was consistent with XRD diffraction pattern results.

## 4 Conclusion

In this study, the marine and freshwater sulfate-reducing bacteria, *D. desulfuricans* and *D. propionicus* were selected to determine their growth characteristics and sulfate reduction abilities; in addition, $Cd^{2+}$ and $Pb^{2+}$ immobilization were compared to explore the mechanism of heavy metal mineralization mediated by microbial sulfate reduction. The results demonstrated that *D. propionicus* exhibited higher sulfate reduction activity than *D. desulfuricans* under $Cd^{2+}$ and $Pb^{2+}$ stress. At a $Cd^{2+}$ concentration of 10 mg/L, the sulfate reduction rates of *D. desulfuricans* and *D. propionicus* reached 61.3% and 88.7%, respectively. Moreover, *D. propionicus* showed twice the tolerance to $Cd^{2+}$ and $Pb^{2+}$ compared to *D. desulfuricans*, along with superior mineralization capacity for both metals. Specifically, *D. propionicus* achieved efficient removal of $Cd^{2+}$ (45.7%–98.7%) at 10–100 mg/L and $Pb^{2+}$ (24.92%–99.9%) at 30–150 mg/L. SRB-mediated immobilization primarily involved the precipitation of heavy metal sulfides (e.g., CdS, PbS) through metabolic reduction of $SO_4^{2-}$. Additionally, $Pb^{2+}$ mineralization generated secondary precipitates such as phosphates and oxides. This study highlights the significant potential of SRB in anaerobic bioremediation for multi-metal systems, owing to their high metal tolerance and diverse precipitation pathways.

## Data availability statement

The original contributions presented in the study are included in the article/Supplementary Material, further inquiries can be directed to the corresponding author/s.

## Author contributions

QC: Conceptualization, Writing – original draft. QM: Formal Analysis, Resources, Writing – review & editing. HW: Conceptualization, Data curation, Writing – review & editing. LZ: Investigation, Methodology, Writing – review & editing. YS: Project administration, Supervision, Writing – original draft, Writing – review & editing.

## Funding

The author(s) declare that financial support was received for the research and/or publication of this article. This work was financially supported by the National Key Research and Development Program of China (2019YFC1805203), the University Synergy Innovation Program of Anhui Province (GXXT-2021-061) and the Funding Plan for Scientific Research Activities of Academic and Technical Leaders and Reserve Candidates in Anhui Province (2021H244).

## Conflict of interest

The authors declare that the research was conducted in the absence of any commercial or financial relationships that could be construed as a potential conflict of interest.

## Generative AI statement

The author(s) declare that no Generative AI was used in the creation of this manuscript.

## Publisher's note



## Supplementary material

The Supplementary Material for this article can be found online at: https://www.frontiersin.org/articles/10.3389/fenvs.2025.1591564/full#supplementary-material

# References


Abdelouas, A., Fattahi, M., Grambow, B., Vichot, L., and Gautier, E. (2002). Precipitation of technetium by subsurface sulfate-reducing bacteria. *Radiochim. Acta* 90 (9-11), 773–777. doi:10.1524/ract.2002.90.9-11_2002.773

Ahluwalia, S. S., and Goyal, D. (2007). Microbial and plant derived biomass for removal of heavy metals from wastewater. *Bioresour. Technol.* 98 (12), 2243–2257. doi:10.1016/j.biortech.2005.12.006

Alam, O., Zheng, X., Du, D., Qiao, X., Dai, L., Li, J., et al. (2024). A critical review on advances in remediation of toxic heavy metals contaminated solids by chemical processes. *J. Environ. Chem. Eng.* 12 (4), 113149. doi:10.1016/j.jece.2024.113149

Alam, R., and Mcphedran, K. (2019). Applications of biological sulfate reduction for remediation of arsenic – a review. *Chemosphere* 222, 932–944. doi:10.1016/j.chemosphere.2019.01.194

Ashraf, S., Ali, Q., Zahir, Z. A., Ashraf, S., and Asghar, H. N. (2019). Phytoremediation: environmentally sustainable way for reclamation of heavy metal polluted soils. *Ecotoxicol. Environ. Saf.* 174, 714–727. doi:10.1016/j.ecoenv.2019.02.068

Belyakova, E. V., Rozanova, E. P., Borzenkov, I. A., Tourova, T. P., Pusheva, M. A., Lysenko, A. M., et al. (2006). The new facultatively chemolithoautotrophic, moderately halophilic, sulfate-reducing bacterium *Desulfovermiculus halophilus* gen. nov., sp nov., isolated from an oil field. *Microbiology* 75 (2), 161–171. doi:10.1134/s0026261706020093

Cardenas, E., Wu, W.-M., Leigh, M. B., Carley, J., Carroll, S., Gentry, T., et al. (2010). Significant association between sulfate-reducing bacteria and uranium-reducing microbial communities as revealed by a combined massively parallel sequencing-indicator species approach. *Appl. Environ. Microbiol.* 76 (20), 6778–6786. doi:10.1128/aem.01097-10

Chen, L., Brookes, P. C., Xu, J., Zhang, J., Zhang, C., Zhou, X., et al. (2016). Structural and functional differentiation of the root-associated bacterial microbiomes of perennial ryegrass. *Soil Biol. & Biochem.* 98, 1–10. doi:10.1016/j.soilbio.2016.04.004

Costa, M. C., and Duarte, J. C. (2005). Bioremediation of acid mine drainage using acidic soil and organic wastes for promoting sulphate-reducing bacteria activity on a column reactor. *Water Air Soil Pollut.* 165 (1-4), 325–345. doi:10.1007/s11270-005-6914-7

Diao, C. Y., Ye, W. Z., Yan, J., Hao, T. W., Huang, L., Chen, Y. H., et al. (2023). Application of microbial sulfate-reduction process for sulfate-laden wastewater treatment: a review. *J. Water Process Eng.* 52, 103537. doi:10.1016/j.jwpe.2023.103537

Dickinson, W. H., Caccavo, F., Olesen, B., and Lewandowski, Z. (1997). Ennoblement of stainless steel by the manganese-depositing bacterium leptothrix discophora. *Appl. Environ. Microbiol.* 63 (7), 2502–2506. doi:10.1128/aem.63.7.2502-2506.1997

Gonzalez-Silva, B. M., Briones-Gallardo, R., Razo-Flores, E., and Celis, L. B. (2009). Inhibition of sulfate reduction by iron, cadmium and sulfide in granular sludge. *J. Hazard. Mater.* 172 (1), 400–407. doi:10.1016/j.jhazmat.2009.07.022

Graham, A. M., Bullock, A. L., Maizel, A. C., Elias, D. A., and Gilmour, C. C. (2012). Detailed assessment of the kinetics of Hg-cell association, Hg methylation, and methylmercury degradation in several *Desulfovibrio* species. *Appl. Environ. Microbiol.* 78 (20), 7337–7346. doi:10.1128/aem.01792-12

Gramp, J. P., Bigham, J. M., Jones, F. S., and Tuovinen, O. H. (2010). Formation of Fe-sulfides in cultures of sulfate-reducing bacteria. *J. Hazard. Mater.* 175 (1-3), 1062–1067. doi:10.1016/j.jhazmat.2009.10.119

Hou, J., Liu, W., Wu, L., Hu, P., Ma, T., Luo, Y., et al. (2017). Modulation of the efficiency of trace metal phytoremediation by *Sedum plumbizincicola* by microbial community structure and function. *Plant Soil* 421 (1-2), 285–299. doi:10.1007/s11104-017-3466-8

Hu, C., Yang, Z., Chen, Y., Tang, J., Zeng, L., Peng, C., et al. (2024). Unlocking soil revival: the role of sulfate-reducing bacteria in mitigating heavy metal contamination. *Environ. Geochem. Health* 46 (10), 417. doi:10.1007/s10653-024-02190-1

Kalwasinska, A., Krawiec, A., Deja-Sikora, E., Golebiewski, M., Kosobucki, P., Brzezinska, M. S., et al. (2020). Microbial diversity in deep-subsurface hot brines of northwest Poland: from community structure to isolate characteristics. *Appl. Environ. Microbiol.* 86 (10), e00252–e00220. doi:10.1128/aem.00252-20

Kim, I. H., Choi, J.-H., Joo, J. O., Kim, Y.-K., Choi, J.-W., and Oh, B.-K. (2015). Development of a microbe-zeolite carrier for the effective elimination of heavy metals from seawater. *J. Microbiol. Biotechnol.* 25 (9), 1542–1546. doi:10.4014/jmb.1504.04067

Koschorreck, M., Bozau, E., Froemmichen, R., Geller, W., Herzsprung, P., and Wendt-Potthoff, K. (2007). Processes at the sediment water interface after addition of organic matter and lime to an acid mine pit lake mesocosm. *Environ. Sci. & Technol.* 41 (5), 1608–1614. doi:10.1021/es0614823

Kurdowski, W., and Bochenek, A. (2012). Three principles of concrete corrosion prevention. *Cem. Wapno Beton* 17 (6), 434–442. Available online at: https://scholar.google.com/scholar_lookup?title=Three+principles+of+concrete+corrosion+prevention&author=Kurdowski,+W.&author=Bochenek,+A.&publication_year=2012&journal=Cem.+Wapno+Beton&volume=17&pages=434%E2%80%93442

Lee, B.-M., and Hur, J. (2016). Adsorption behavior of extracellular polymeric substances on graphene materials explored by fluorescence spectroscopy and two-dimensional fourier transform infrared correlation spectroscopy. *Environ. Sci. & Technol.* 50 (14), 7364–7372. doi:10.1021/acs.est.6b01286

Le Pape, P., Battaglia-Brunet, F., Parmentier, M., Joulian, C., Gassaud, C., Fernandez-Rojo, L., et al. (2017). Complete removal of arsenic and zinc from a heavily contaminated acid mine drainage via an indigenous SRB consortium. *J. Hazard. Mater.* 321, 764–772. doi:10.1016/j.jhazmat.2016.09.060

Li, B., Xu, R., Sun, X., Han, F., Xiao, E., Chen, L., et al. (2021). Microbiome-environment interactions in antimony-contaminated rice paddies and the correlation of core microbiome with arsenic and antimony contamination. *Chemosphere* 263, 128227. doi:10.1016/j.chemosphere.2020.128227

Liao, L., Li, Q., Yang, Y., Xu, R., and Zhang, Y. (2024). Immobilization behavior and mechanism of $Cd^{2+}$ by sulfate-reducing bacteria in anoxic environments. *Water* 16 (8), 1086. doi:10.3390/w16081086

Liu, Z., Osterlund, T., Hou, J., Petranovic, D., and Nielsen, J. (2013). Anaerobic α-amylase production and secretion with fumarate as the final electron acceptor in *saccharomyces cerevisiae*. *Appl. Environ. Microbiol.* 79 (9), 2962–2967. doi:10.1128/aem.03207-12

Mallhi, Z. I., Rizwan, M., Mansha, A., Ali, Q., Asim, S., Ali, S., et al. (2019). Citric acid enhances plant growth, photosynthesis, and phytoextraction of lead by alleviating the oxidative stress in castor beans. *Plants-Basel* 8 (11), 525. doi:10.3390/plants8110525

Meulepas, R. J. W., Jagersma, C. G., Khadem, A. F., Buisman, C. J. N., Stams, A. J. M., and Lens, P. N. L. (2009). Effect of environmental conditions on sulfate reduction with methane as electron donor by an eckernforde bay enrichment. *Environ. Sci. & Technol.* 43 (17), 6553–6559. doi:10.1021/es900633c

Ohfuji, H., and Rickard, D. (2006). High resolution transmission electron microscopic study of synthetic nanocrystalline mackinawite. *Earth Planet. Sci. Lett.* 241 (1-2), 227–233. doi:10.1016/j.epsl.2005.10.006

Parshina, S. N., Sipma, J., Nakashimada, Y., Henstra, A. M., Smidt, H., Lysenko, A. M., et al. (2005). *Desulfotomaculum carboxydivorans* sp nov., a novel sulfate-reducing bacterium capable of growth at 100 % CO. *Int. J. Syst. Evol. Microbiol.* 55, 2159–2165. doi:10.1099/ijs.0.63780-0

Picard, A., Gartman, A., Clarke, D. R., and Girguis, P. R. (2018). Sulfate-reducing bacteria influence the nucleation and growth of mackinawite and greigite. *Geochimica Cosmochimica Acta* 220, 367–384. doi:10.1016/j.gca.2017.10.006

Qian, J., Zhu, X., Tao, Y., Zhou, Y., He, X., and Li, D. (2015). Promotion of $Ni^{2+}$ removal by masking toxicity to sulfate-reducing bacteria: addition of citrate. *Int. J. Mol. Sci.* 16 (4), 7932–7943. doi:10.3390/ijms16047932

Rehman, A., Zhong, S., Du, D., Zheng, X., Arif, M. S., Ijaz, S., et al. (2025a). Unveiling the microplastics degradation and its transformative effects on soil nutrient dynamics and plant health - a systematic review. *Sustain. Prod. Consum.* 54, 25–42. doi:10.1016/j.spc.2024.12.018

Rehman, A., Zhong, S., Du, D., Zheng, X., Ijaz, S., Haider, M. I. S., et al. (2025b). Unveiling sources, contamination, and eco-human health implications of potentially toxic metals from urban road dust. *Sci. Rep.* 15 (1), 10673. doi:10.1038/s41598-025-95205-5

Roychoudhury, A. N., Van Cappellan, P., Kostka, J. E., and Viollier, E. (2003). Kinetics of microbially mediated reactions: dissimilatory sulfate reduction in saltmarsh sediments (Sapelo Island, Georgia, USA). *Estuar. Coast. Shelf Sci.* 56 (5-6), 1001–1010. doi:10.1016/s0272-7714(02)00325-6

Sievert, S. M., and Kuever, J. (2000). *Desulfacinum hydrothermale* sp nov., a thermophilic, sulfate-reducing bacterium from geothermally heated sediments near Milos Island (Greece). *Int. J. Syst. Evol. Microbiol.* 50 (3), 1239–1246. doi:10.1099/00207713-50-3-1239

Siswoyo, E., Qoniah, I., Lestari, P., Fajri, J. A., Sani, R. A., Sari, D. G., et al. (2019). Development of a floating adsorbent for cadmium derived from modified drinking water treatment plant sludge. *Environ. Technol. & Innovation* 14, 100312. doi:10.1016/j.eti.2019.01.006

Somenahally, A. C., Hollister, E. B., Yan, W., Gentry, T. J., and Loeppert, R. H. (2011). Water management impacts on arsenic speciation and iron-reducing bacteria in contrasting rice-rhizosphere compartments. *Environ. Sci. & Technol.* 45 (19), 8328–8335. doi:10.1021/es2012403

Song, S., Han, Y., Zhang, Y., Ma, H., Zhang, L., Huo, J., et al. (2019). Protective role of citric acid against oxidative stress induced by heavy metals in *Caenorhabditis elegans*. *Environ. Sci. Pollut. Res.* 26 (36), 36820–36831. doi:10.1007/s11356-019-06853-w

Southam, G., and Saunders, J. A. (2005). The geomicrobiology of ore deposits. *Econ. Geol.* 100 (6), 1067–1084. doi:10.2113/100.6.1067

Thatoi, H., Das, S., Mishra, J., Rath, B. P., and Das, N. (2014). Bacterial chromate reductase, a potential enzyme for bioremediation of hexavalent chromium: a review. *J. Environ. Manag.* 146, 383–399. doi:10.1016/j.jenvman.2014.07.014

Venceslau, S. S., Da Silva, S. M., Marques, M. C., Grein, F., Ramos, A. R., and Pereira, I. a.C. (2011). A comparative genomic analysis of energy metabolism in sulfate reducing bacteria and archaea. *Front. Microbiol.* 2, 69. doi:10.3389/fmicb.2011.00069

Wang, C. L., Maratukulam, P. D., Lum, A. M., Clark, D. S., and Keasling, J. D. (2000). Metabolic engineering of an aerobic sulfate reduction pathway and its application to precipitation of cadmium on the cell surface. *Appl. Environ. Microbiol.* 66 (10), 4497–4502. doi:10.1128/aem.66.10.4497-4502.2000

Wang, X., Ye, Z., Li, B., Huang, L., Meng, M., Shi, J., et al. (2014). Growing rice aerobically markedly decreases mercury accumulation by reducing both Hg bioavailability and the production of MeHg. *Environ. Sci. & Technol.* 48 (3), 1878–1885. doi:10.1021/es4038929

Wu, Z., Firmin, K. A., Cheng, M., Wu, H., and Si, Y. (2022). Biochar enhanced Cd and Pb immobilization by sulfate-reducing bacterium isolated from acid mine drainage environment. *J. Clean. Prod.* 366, 132823. doi:10.1016/j.jclepro.2022.132823

Xu, H., Liu, Y., Yang, B., Jia, L., Li, X., Li, F., et al. (2021a). Inhibitory effect of released phosphate on the ability of nano zero valent iron to boost anaerobic digestion of waste-activated sludge and the remediation method. *Chem. Eng. J.* 405, 126506. doi:10.1016/j.cej.2020.126506

Xu, J., Zhang, X., Sun, C., He, H., Dai, Y., Yang, S., et al. (2018). Catalytic degradation of diatrizoate by persulfate activation with peanut shell biochar-supported nano zero-valent iron in aqueous solution. *Int. J. Environ. Res. Public Health* 15 (9), 1937. doi:10.3390/ijerph15091937

Xu, L., Wang, Y., Zhou, D., Chen, M.-Y., Yang, X.-J., Ye, X.-M., et al. (2021b). Bio-metabolism-driven crystalline-engineering of CdS quantum dots for highly active photocatalytic $H^2$ evolution. *Chemistryselect* 6 (15), 3702–3706. doi:10.1002/slct.202100591

Yin, K., Wang, Q., Lv, M., and Chen, L. (2019). Microorganism remediation strategies towards heavy metals. *Chem. Eng. J.* 360, 1553–1563. doi:10.1016/j.cej.2018.10.226

Zhang, H. B., Duan, C. Q., Shao, Q. Y., Ren, W. M., Sha, T., Cheng, L. Z., et al. (2004). Genetic and physiological diversity of phylogenetically and geographically distinct groups of *Arthrobacter* isolated from lead-zinc mine tailings. *Fems Microbiol. Ecol.* 49 (2), 333–341. doi:10.1016/j.femsec.2004.04.009

Zhang, S., Ke, C., Jiang, M., Li, Y., Huang, W., Dang, Z., et al. (2023). S(-II) reactivates $Cd^{2+}$ stressed Shewanella oneidensis via promoting low-molecular-weight thiols synthesis and activating antioxidant defense. *Environ. Pollut.* 327, 121516. doi:10.1016/j.envpol.2023.121516

Zhang, Z., Zhang, C., Yang, Y., Zhang, Z., Tang, Y., Su, P., et al. (2022). A review of sulfate-reducing bacteria: metabolism, influencing factors and application in wastewater treatment. *J. Clean. Prod.* 376, 134109. doi:10.1016/j.jclepro.2022.134109

Zhao, Q., Li, X., Xiao, S., Peng, W., and Fan, W. (2021). Integrated remediation of sulfate reducing bacteria and nano zero valent iron on cadmium contaminated sediments. *J. Hazard. Mater.* 406, 124680. doi:10.1016/j.jhazmat.2020.124680

Zheng, R., Wu, S., and Sun, C. (2021). *Pseudodesulfovibrio cashew* sp. nov., a novel deep-sea sulfate-reducing bacterium, linking heavy metal resistance and sulfur cycle. *Microorganisms* 9 (2), 429. doi:10.3390/microorganisms9020429

Zheng, X., Alam, O., Zhou, Y., Du, D., Li, G., and Zhu, W. (2024a). Heavy metals detection and removal from contaminated water: a critical review of adsorption methods. *J. Environ. Chem. Eng.* 12 (6), 114366. doi:10.1016/j.jece.2024.114366

Zheng, X., Lin, H., Du, D., Li, G., Alam, O., Cheng, Z., et al. (2024b). Remediation of heavy metals polluted soil environment: a critical review on biological approaches. *Ecotoxicol. Environ. Saf.* 284, 116883. doi:10.1016/j.ecoenv.2024.116883

Zhong, S., Dai, L. Y., Xu, H., Yang, X. C., Zheng, X. J., and Wang, S. (2024a). Highly porous carbon with selective transformation of nitrogen groups boosts the capacitive performance through boric acid template assisted strategy. *J. Energy Storage* 97, 112867. doi:10.1016/j.est.2024.112867

Zhong, S., Xu, H., Zheng, X. J., Li, G. L., and Wang, S. (2024b). High-value conversion of invasive plant into nitrogen-doped porous carbons for high-performance supercapacitors. *J. Of Anal. Appl. Pyrolysis* 183, 106814. doi:10.1016/j.jaap.2024.106814

Zhou, Q., Chen, Y., Yang, M., Li, W., and Deng, L. (2013). Enhanced bioremediation of heavy metal from effluent by sulfate-reducing bacteria with copper-iron bimetallic particles support. *Bioresour. Technol.* 136, 413–417. doi:10.1016/j.biortech.2013.03.047

Zhuang, Q., Guo, C., Zhang, S., Ren, M., Deng, Y., Wang, C., et al. (2024). Effect of $Cd^{2+}$ and $Cu^{2+}$ on *Desulfovibrio vulgaris* strain ATCC 7757: insights from sulfur isotope fractionation. *J. Environ. Chem. Eng.* 12 (6), 114545. doi:10.1016/j.jece.2024.114545